Available online at www.sciencedirect.com

ScienceDirect

Energy Procedia 49 (2014) 790 – 799

Energy Procedia

SolarPACES 2013

A new thermocline-PCM thermal storage concept for CSP plants. Numerical analysis and perspectives

P. A. Galione[a,c], C. D. Pérez-Segarra[a], I. Rodríguez[a], O. Lehmkuhl[a,b], J. Rigola[a]*

[a]*Heat and Mass Transfer Technological Center (CTTC) Universitat Politècnica de Catalunya – BarcelonaTech, ETSEIAT, Colom 11, Terrassa 08222, Spain*

[b]*Termo Fluids S.L., Avda. Jacquard 97 1-E, Terrassa 08222, Spain*

[c] *Instituto de Ingeniería Mecánica y Producción Industrial (IIMPI), Facultad de Ingeniería, Universidad de la República (UdelaR), Julio Herrera y Reissig 565, Montevideo 11300, Uruguay*

Abstract

Thermocline storage concept has been considered for more than a decade as a possible solution to reduce the huge cost of the storage system in CSP plants. However, one of the drawbacks of this concept is the decrease in its performance throughout the time. The objective of this paper is to present a new thermocline-PCM storage concept which aims at circumventing this issue. The concept proposed is built of different solid filler materials and encapsulated PCMs combined into a multi-layer storage tank with molten salt as heat transfer fluid. The performance evaluation of each of the prototypes proposed is virtually tested by means of a detailed numerical methodology which considers the heat transfer and fluid dynamics phenomena present in these devices. The virtual tests carried out are designed so as to take into account several charging and discharging cycles until equilibrium is achieved, i.e. the same amount of energy stored in the charging phase is delivered in the discharge. As a result, the dependence of the storage capacity on the PCMs temperatures, the total energy stored/released, as well as the efficiencies of the storing process have been compared for the different thermocline, PCM-only and multi-layered thermocline-PCM configurations. Based on this analysis the selection of the best option for a given case/plant is proposed.

Selection and peer review by the scientific conference committee of SolarPACES 2013 under responsibility of PSE AG.
Final manuscript published as received without editorial corrections.

Keywords: Thermal energy storage (TES); thermocline; PCM; numerical simulation; CSP

* Corresponding author. Tel.: +34-937398192; fax: +34-937398920.
*E-mail address:*cttc@cttc.upc.edu

Selection and peer review by the scientific conference committee of SolarPACES 2013 under responsibility of PSE AG.
Final manuscript published as received without editorial corrections.
doi:10.1016/j.egypro.2014.03.086

1. Introduction

Thermal energy storage systems are an essential feature to make an efficient use of solar energy due to the inherent intermittence of this energy source. These systems allow making use of thermal energy —accumulated in hours of high solar radiation— in moments of lower solar radiation, reducing the mismatch between the supply and demand of the energy.

For concentrated solar power plants (CSP) the current standard thermal storage system is the two-tank molten salt. Thermocline storage system has also been considered as an alternative that would result in lower costs, since it consists of a single tank instead of two and a high amount of the expensive molten salt could be replaced by a cheaper filler material. This system relies on the principle of stratification, which occurs in a fluid having temperature gradients, under the action of gravitational force. The hot fluid, which has a lower density than the cold fluid, is pushed upwards by the buoyancy force, while the low temperature fluid is displaced downwards. Therefore, the hot fluid is placed in the upper part of a tank, while the colder fluid stays at the bottom. A vertical temperature gradient is formed, which is called *Thermocline*. A low-cost filler material is used to displace part of the higher-cost heat transfer fluid, as well as to maintain the thermal gradient. This material can be quartzite rocks, granite, sand, asbestos-containing wastes [1], etc.

Encapsulated phase change materials (PCM) can also be used to store energy, using less storage material than would be used with a sensible energy storage medium. The resulting storage device should be lighter and smaller, and hopefully cheaper, than one that only makes profit of sensible energy changes. Tanks filled with encapsulated PCM are being studied as a form of thermal storage devices.

This work studies a new concept of thermocline-like storage device, which consists in combining different filler materials –low-cost solid and different encapsulated PCM– appropriately chosen and placed inside the tank in a multi-layer manner. Numerical simulations have been carried out in order to test the thermal performance and optimize the design of the storage system, as well as to compare it against different thermocline-like designs such as “pure” thermocline [2], single encapsulated PCM and cascaded-PCM [3] concepts. The tank dimensions are adopted from those presented in [2], as well as the solid filler material considered.

The operation of the storage system consists of charging and discharging processes. The tank is charged by extracting cold fluid from the bottom, heating it with the external heat source (e.g. solar field, heat exchanger) and returning it to the top of the tank. The discharge is carried out the opposite way, i.e. extracting hot fluid from the top, cooling it in the external heat sink (e.g. power block) and returning it to the tank by its bottom.

2. Mathematical modelling and numerical implementation

Mass, momentum and energy conservation equations have to be solved in order to be able to simulate the thermal behavior of a thermocline-like tank. Some simplifying assumptions are made and empirical correlations are used. Most relevant assumptions are:

- One-dimensional fluid flow and temperature distribution (in the flow direction).
- One-dimensional heat transfer in filler particles/capsules (radial direction).
- Spherical shape of filler particles/capsules.
- Constant density of both fluid and filler bed materials (solid and PCM).
- Heat conduction in flow direction is neglected.
- Heat conduction between different filler material particles/capsules is not considered.
- Negligible radiation transfer.

The one-dimensionality in the fluid results in an axially-varying fluid temperature map. In the filler particles/capsules, a radial variation of the temperature is assumed, which also depends on the axial position in the tank.

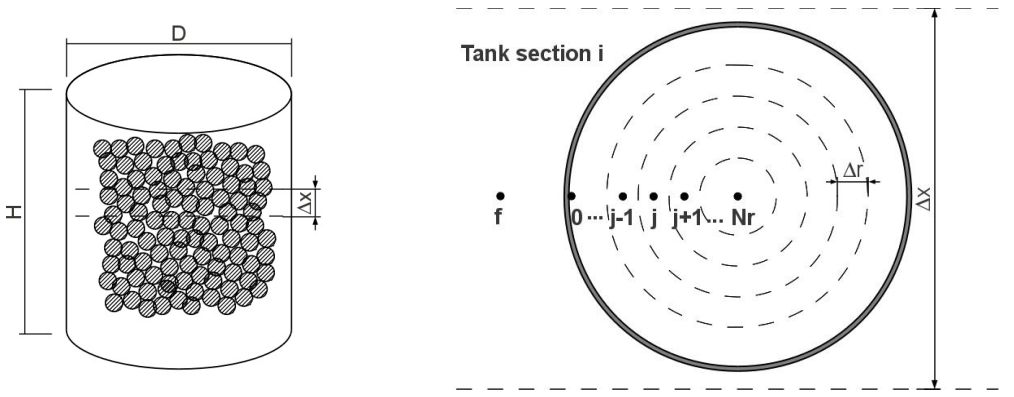

Fig. 1. (a) Sketch representing the cylindrical container with the PCM capsules packed in a random fashion; (b) discretization details of the tank and of a representative particle/capsule, indicating the sub-indices used for tank sections (*i*) and capsule control volumes (*j*).

For determining the temperature of the fluid and of the filler material, the energy conservation equations are discretized using the Finite Volume Method. The tank is divided in transversal cylindrical sections of equal height (Δx), as sketched in Fig. 1(a). In each tank section, a single particle/capsule needs to be simulated, as all are affected by the same fluid temperature, due to one-dimensionality assumption. This filler particule, assumed as spherical, is discretized in the radial direction in *Nr* control volumes, as shown in Fig. 1(b).

2.1. Fluid flow equations:

The energy and momentum balances of the fluid in a tank section *i* result in:

$$\rho_f \varepsilon_i V_i C_{p,f} \frac{dT_{f,i}}{dt} = -\dot{m} C_{p,f} \left(T_{f,i}^{out} - T_{f,i}^{in} \right) - n_{cap,i} \frac{\left(T_{f,i} - T_{i,0} \right)}{R_{conv,i} + R_{cond}} - U_{amb} A_{w,i} \left(T_{f,i} - T_{amb} \right) \tag{1}$$

$$\frac{\Delta p_i}{\Delta x_i} = \left(\frac{4.17}{\mathrm{Re}_{1,i}} + 0.29 \right) \frac{\rho_f v^2 \left(1-\varepsilon_i\right) 6}{d_{p,i} \varepsilon_i^{\,3}} \tag{2}$$

where $\mathrm{Re}_{1,i} = \dfrac{\rho_f v d_{p,i}}{\left(1-\varepsilon_i\right) 6 \mu_f}$ (spherical particles) and $v = \dfrac{\dot{m}}{\rho_f A_t}$

Sub-index *i* indicates the tank section where the temperature is being calculated, while *f* indicates that the property/variable corresponds to the fluid. ρ is the density; ε is the porosity of the bed; *V* is the tank section volume; C_p the specific heat; $\dot{m}$ the mass flux; n_{cap} the number of capsules contained in the section; R_{conv} and R_{cond} are the thermal resistances due to convection between fluid and capsule and conduction through the capsule shell, respectively. R_{conv} calculation requires the fluid-to-bed Nusselt number, which is calculated using the correlation obtained from [4]. U_{amb} is the convection coefficient between the ambient and the fluid and A_w the surface area of the tank wall. T^{out} and T^{in} are the temperatures of outgoing and ingoing flows from and into the control volume, respectively; $T_{i,0}$ the temperature of the internal surface of the particles/capsules (boundary node) and T_{amb} the temperature of ambient air. *p* is the pressure (sum of the gauge and elevation pressures) of the fluid, *x* the axial

position in the tank, d_p the diameter of particle/capsule, μ_f the dynamic viscosity of the fluid and A_t the transversal surface area of the tank. Eq. 2 is the Ergun correlation for packed beds [5].

The energy balance for the filler material (PCM capsules or solid particles) remains:

$$\textit{(Inner nodes)} \quad \rho_{filler} V_{i,j} \frac{\partial h_{i,j}}{\partial t} = \left(k_{filler} A \frac{\partial T}{\partial r} \right)_{i,j-\frac{1}{2}} - \left(k_{filler} A \frac{\partial T}{\partial r} \right)_{i,j+\frac{1}{2}} \tag{3}$$

$$\textit{(Boundary node)} \quad \rho_{filler} V_{i,0} \frac{\partial h_{i,0}}{\partial t} = \frac{\left(T_{f,i} - T_{i,0} \right)}{R_{conv,i} + R_{cond}} - \left(k_{filler} A \frac{\partial T}{\partial r} \right)_{i,\frac{1}{2}} \tag{4}$$

where sub-index *j* indicates the control volume *j* of the simulated capsule*; h* is the specific total enthalpy (sensible and latent) and k_{filler} is the thermal conductivity of the filler material. Sub-indices *j-1/2* and *j+1/2* indicate the boundaries of control volume *j*, facing the shell and the center of the sphere, respectively. *A* is the surface area of the control volume (inside the sphere) and *r* indicates the radial direction.

To solve these equations, it is necessary to define a relation between the enthalpy and the temperature of the filler materials (solid and/or PCM). These are similar to those presented in [6] and are detailed next.

2.2. Enthalpy – temperature relations for the filler material (solid and/or PCM):

$$h - h_0 = C_{p,s} \left(T - T_0 \right), \qquad T \le T_s \tag{5}$$

$$h - h_0 = C_{p,s} \left(T - T_0 \right) + fL, \qquad T_s < T \le T_{sl} \tag{6}$$

$$h - h_0 = C_{p,l} \left(T - T_{sl} \right) + C_{p,s} \left(T_{sl} - T_0 \right) + fL, \qquad T_{sl} < T \le T_l \tag{7}$$

$$h - h_0 = C_{p,l} \left(T - T_{sl} \right) + C_{p,s} \left(T_{sl} - T_0 \right) + L, \qquad T_l < T \tag{8}$$

$$f = \frac{T - T_s}{T_l - T_s} \tag{9}$$

Sub-index 0 here indicates reference values, while s and l indicate solid and liquid phases, respectively. T_s and T_l are the solidus and liquidus temperatures, respectively; while T_{sl} indicates the temperature in the phase change range beyond which the material has a mostly liquid behavior, and below which it behaves mostly as solid. *f* is the liquid fraction, whose values go from 0 (pure solid) to 1 (pure liquid) and *L* is the latent heat of fusion. Since T_s and T_l are not the same, these equations are meant to model PCMs with a fusion temperature range. However, taking a very narrow temperature range, fixed fusion temperature PCMs can also be modeled with this approach. Hence, a unique value of *h* exists for each value of *T*, and the energy balance equations may be expressed with *T* as the only variable.

It should be noted that with this strategy an explicit tracking of the liquid-solid interface is avoided, since its location is implicitly determined by values of *f* between 0 and 1 (indicating a solid-liquid mixture).

2.3. Discretization details

For the temporal discretization a 1st order fully implicit scheme is chosen. Furthermore, an upwind-like scheme is used to determine the temperatures of the flow entering and leaving each section (T_i^{in} and T_i^{out}, respectively). Thus,

the temperature of the fluid entering section of tank *i* (T_i^{in}, coming from section *i-1*) becomes the same as the temperature of the fluid in section *i-1* (i.e. $T_{f,i-1}$), and the temperature of the fluid leaving section *i* (T_i^{out}, going to section *i+1*) is taken equal to $T_{f,i}$. This scheme allows to adopt a step by step method to solve the entire tank, first solving the section where the inlet is placed (in the top or bottom of the tank), then the next section downstream, and so on advancing in the direction of the flow, until the end of the tank is reached; and this is done only once per time step, without needing further iterations.

In each section, fluid and filler material temperatures have to be solved. The final matrix of coefficients derived from the system of equations in each container section has a tri-diagonal pattern. This allows the usage of a TDMA algorithm to solve the linear system. This formulation is implemented in a simple computer code intended to simulate the behavior in charging and discharging modes of the whole energy storage system.

3. Model validation

To validate the model presented in the previous section, the experimental work of Pacheco et al. [2] is used. There, a thermocline tank filled with quartzite rock and sand was tested using molten salt as the heat transfer fluid. Apart from thermal cycling tests intended to evaluate the endurance of different filler materials, they carried out tests aimed to measure the performance of a pilot scale device under operating conditions similar to those of a parabolic trough solar power plant. In this work, results from a discharge cycle are used to validate our model.

In the experiments carried out by Pacheco et al. [2], a cylindrical tank of 6.1 m height by 3.0 m diameter was used. Several thermocouples were placed throughout the vertical axis of the tank, as well as radially, at some selected vertical positions. Initially, the temperatures of filler material and fluid were around 390ºC. The tests consisted in drawing hot fluid off the top of the tank, pumping it through a forced air salt cooler to reject the heat from the salt and returning it to the bottom of the tank at a temperature around 290ºC.

Numerical tests have been performed in order to reproduce the experimental results obtained in [2]. Due to the lack of complete information of the experimental tests, some data have been extracted from reference [7].

The tank has been discretized axially in 60 sections; each simulated filler particle divided radially in 10 control volumes and the time step was of around 10 seconds. These parameters were verified in the sense of producing grid and time step independent results.

The initial state adopted in the simulations is the temperature map obtained from the experimental measures at time 11:30, extracted from [2]. Filler material and fluid inside the tank are assumed to be at thermal equilibrium at this initial state. Ambient losses are neglected.

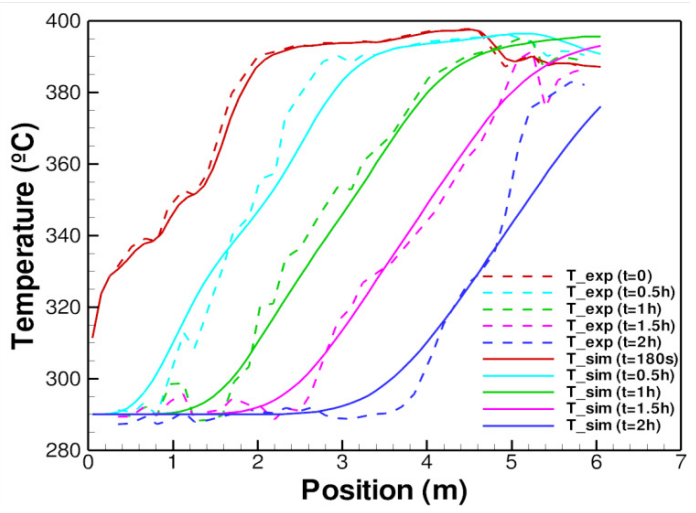

Fig. 2. Numerical simulation results (solid lines) and experimental results (dashed lines, from [2]).

Simulation results are presented in Fig. 2. It can be observed that the thermal gradient is reproduced and that it moves towards the top as the discharge proceeds. Good agreement between experimental and numerical results is observed. However, some differences are encountered which may be due to several causes. Firstly, experimental measurements inherently carry some uncertainties. Secondly, not all the input data needed for the numerical simulations was available from the work of Pacheco et al. [2], so it had to be taken from other sources [7]. Thirdly, the simplifying assumptions –as well as the empirical correlation for the convective transfer used in Eq. 1– made in the development of the model presented here, inevitably introduce some kind of errors.

4. Evaluation of different solutions

In this section, different configurations of thermocline-like storage systems are considered and compared ("pure" thermocline, single PCM, multilayered solid-PCM, cascaded PCM). Fig. 3 shows a sketch of the multilayered configuration. The following operating conditions are assumed:

1. The geometry of the tank and the operating conditions are the same for all the cases. Tank dimensions and fluid inlet temperatures are the same as those of the experiment of Pacheco et al. [2].
2. The operation time is **not** fixed.
3. Instead, outlet **temperature limits** are imposed, which will force the stop of each process (charge or discharge). For the charge process, outlet temperature has to be between the minimum temperature and a predefined set temperature, which cannot be surpassed. For the discharge process, another set temperature is predefined, restricting the outlet temperature to be between this set and the maximum operating temperature. These temperature intervals will be referred to as "admissible" temperature ranges. Here, both admissible ranges have been assumed to be 15% of the maximum temperature interval (100ºC); e.g. in the charging phase, the outlet fluid temperature is allowed to be between 290ºC and 305ºC.
4. Several consecutive charge and discharge cycles are simulated until thermal equilibrium is reached between consecutive processes, i.e. until the same energy that is stored in the charge is released in the discharge.
5. Ambient losses are neglected ($U_{amb} = 0$ in Eq. 1).

Items 2 and 3 reflect that usually, the operating time of a thermal storage system is limited by the temperature of the fluid coming out. For example, in a solar thermal power facility, the outlet temperature in the discharge process is limited by the minimum temperature that is admissible for the fluid feeding the power block. Similarly, for the charging process, the outlet temperature is limited by the restriction in the temperature of the fluid coming into the solar receivers. Therefore, both the operating time and the stored energy are determined by the level of temperatures attained by the outlet fluid in the charge and discharge processes. Furthermore, as the admissible temperature intervals for both charge and discharge processes are quite narrow, outlet fluid temperatures for all the cases here studied are very similar. Therefore, a higher operation time is directly related to the stored (or released) energy.

The fact of reaching a thermal equilibrium between processes ensures that the obtained results are independent of the initial state of the tank filler material and HTF.

In Table 1, a code for each case/configuration is defined. The presented cases can be classified according to the filler material/s used as: "pure" thermocline (A); single PCM (B); multilayered solid-PCM (C and D), where both solid filler material and encapsulated PCM are included; and cascaded PCM (F). Percentages between brackets indicate the portion of total height occupied by each filler material. It should be noted that the chosen PCMs are theoretical PCM with the same thermal properties as KOH but with different fusion temperatures; except from case B1, where real KOH is considered (fusion temperature = 360ºC). This procedure has been adopted in order to account for the variations in performance exclusively due to the change in the fusion temperature of the PCM.

Table 2 shows, for each case, the mass of solid filler material, PCM and heat transfer fluid (HTF, i.e. molten salt). Table 3 presents data of the maximum amount of energy that could be stored in each of the configurations, taking into account both sensible and latent energy contributions with a temperature difference of 100ºC.

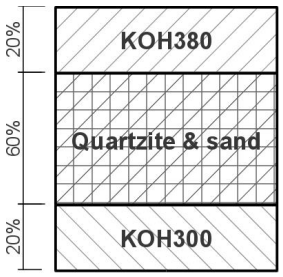

Fig. 3. Sketch of a multilayered solid-PCM configuration. Picture corresponds to case C1.

Table 1. Codification of the configurations. Materials KOHXXX (XXX is a 3 digit number) are theoretical PCMs with fusion temperatures indicated by the number XXX (e.g. 300ºC), whose thermal properties are equal to those of KOH (whose fusion temperature is 360ºC). The order at which the materials are indicated is the order at which they are collocated inside the tank, from top to bottom. Between brackets, the proportion of the tank height occupied by each material is indicated.

Filler materials	Code
Quarzite rock & sand (Qu) (100%)	A
KOH (100%)	B1
KOH380 (100%)	B2
KOH300 (100%)	B3
KOH380–Qu–KOH300 (20%-60%-20%)	C1
KOH380–Qu–KOH300 (40%-20%-40%)	C2
KOH380–Qu–KOH340-Qu-KOH300 (20%-25%-10%-25%-20%)	D
KOH380–KOH370-KOH340–KOH310-KOH300 (32%-15%-6%-15%-32%)	F1
KOH380–KOH370-KOH340–KOH310-KOH300 (32%-12%-13%-12%-32%)	F2

Table 2. Mass confined inside the tank for the different test cases

MASS DATA	A	B1	B2	B3	C1	C2	D	F1	F2
Mass of PCM (ton)	0	51.0	51.0	51.0	20.4	40.8	25.5	51.0	51.0
Mass of Quartzite & sand (ton)	84.1	0	0	0	50.4	16.8	42.0	0	0
Mass of confined HTF (ton)	17.8	27.5	27.5	27.5	21.7	25.5	22.6	27.5	27.5
Total mass (ton)	101.9	78.5	78.5	78.5	92.5	83.2	90.2	78.5	78.5

Table 3. Maximum storable energy for the different test cases

STORABLE ENERGY (MWh)	A	B1	B2	B3	C1	C2	D	F1	F2
Filler material	1.94	3.80	3.80	3.80	2.68	3.43	2.87	3.80	3.80
Confined HTF	0.74	1.15	1.15	1.15	0.90	1.06	0.94	1.15	1.15
Total (filler + HTF)	2.68	4.94	4.94	4.94	3.59	4.49	3.81	4.94	4.94

Table 4. Operating conditions

Temp. hot molten salt (ºC)	Temp. cold molten salt (ºC)	Limit outlet Temp. Charge process (ºC)	Limit outlet Temp. Discharge process (ºC)	Molten salt mass flow (kg/s)
390	290	305	375	5.54

Table 5. Thermo-physical properties of the different materials

	ρ (kg/m3)	C_{ps} (J/kg K)	C_{pl} (J/kg K)	k_s (W/m K)	k_l (W/m K)	L (J/kg)
Quarzite rock & sand (Qu)	2500	830	-	5.69	-	-
PCM (KOHXXX)	2040	1340	1340	0.5	0.5	1.34×10^5
Molten salt	1873.8	-	1501.5	-	$0.443 + 1.9 \times 10^{-4} \times T(ºC)$	-

Table 4 shows the operating conditions and Table 5 the physical properties used in the simulations. The solid filler material adopted here is a mixture of quartzite rock and sand, as in [2], whose properties have been extracted from [7]. The properties of all the PCM considered are those of KOH [3], except from their fusion temperatures, which have been artificially chosen as explained in Table 1. Molten salt properties have been taken from [8].

4.1. Results

Table 6 shows the thermal performance results of each of the cases previously defined. Case A ("pure" thermocline) is shown to behave quite poorly in terms of stored energy when compared against the rest of the cases (with exception of case B1). The stored energy at thermal equilibrium is 1.45 MWh, which is lower than half the theoretically storable energy for the operation conditions of Table 4 and around half the design capacity stated in the work of Pacheco et al. [2] (2.3 MWh). This is due to the thermocline degradation throughout the several charging-discharging cycles. This degradation has been observed in the temperature maps and exchanged energy of the numerical simulations for consecutive cycles. Fig. 4 shows the temperature maps of charge and discharge processes at various instants, for case A. It can be observed that charge and discharge maps are symmetric, which is a result of having reached equilibrium between consecutive processes.

Table 6. Performance results

RESULTS	A	B1	B2	B3	C1	C2	D	F1	F2
Storage Time (h)	1.45	1.18	2.48	2.65	3.19	3.35	2.06	3.51	2.26
Stored Energy in *Filler* material (MWh)	0.84	0.60	1.32	1.32	1.82	1.83	1.20	2.02	1.31
Stored Energy in *Total* (MWh)	1.17	0.95	2.02	2.02	2.44	2.57	1.57	2.69	1.73
Total Stored Energy / *Storable* Energy in *Total* (%)	43.7	19.1	40.8	40.8	68.1	57.1	41.3	54.4	35.0
Effective mass of PCM changing phase (%)	-	2.6	9.9	9.9	63.8	33.7	49.0	49.2	34.3
Pressure losses due to filler bed (Pa)*	~200	<100	<100	<100	~100	<100	~100	<100	<100

* The pressure losses are not indicated as a single value because they change during the simulation, due to the change in dynamic viscosity with the temperature.

Case B1, filled with a single encapsulated PCM with a fusion temperature of 360ºC, which is outside both admissible-temperature ranges (see Table 4), results in an even lower stored/released energy at the equilibrium. However, when looking at the results obtained with cases B2 and B3, which also include a single encapsulated PCM as filler material –only differing in the fusion temperature, but both inside one of the two admissible temperature ranges– it is observed an increase in stored energy (and storage time). In case B2 (B3) the PCM close to the top (bottom) is seen to be the one changing phase between processes. These layers of PCM work as a thermal "buffer", maintaining the outlet fluid temperature close to the fusion temperature (B2: 380ºC; B3: 300ºC), which is an admissible temperature for one of the processes. This allows a high temperature jump of most of the filler material and heat transfer fluid inside the tank.

Cases C1 and C2 are both multi-layered solid-PCM tanks with two different PCM collocated at both ends of the tank and solid filler material (quartzite rocks & sand) in between. The PCM with the higher fusion temperature is placed at the top (hot zone) and the lower fusion temperature PCM at the bottom (cold zone). Both PCM have fusion temperatures contained in the corresponding admissible range. Results for these cases show a significant improvement with respect to previous cases. The "buffering" effect of the PCM at both ends can be appreciated in

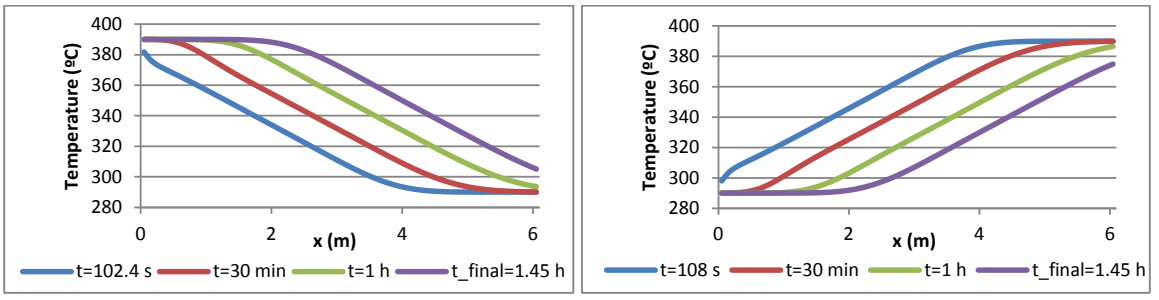

Fig. 4. Case A (Thermocline). Fluid temperature maps at various instants. Left: Charge process, x indicates the distance from the top of the tank. Right: Discharge; x indicates the distance from the bottom of the tank.

Fig. 5. Both the stored/released energy and the efficiency in the utilization of the thermal capacity of the storage tank are higher. Although C1 stores less energy than C2, the efficiency in the utilization of thermal capacity is higher in the former.

Case D is similar to C1, replacing some portion of solid filler material with a PCM with fusion temperature equal to the mean between inlet temperatures of charge and discharge (290ºC and 390ºC, respectively). This replacement is detrimental to the resulting stored energy. The presence of the middle PCM imposes a temperature buffer that makes the fluid to be close to the fusion temperature of this PCM, preventing a high thermal jump of the whole filler material. The thermal jump is roughly the temperature difference between consecutive PCM, i.e. 40ºC.

Cases F1 and F2 are both cascaded PCM cases [3], with no solid filler material (only PCM). The difference between both cases is in the quantity of the three middle PCM layers included. A high difference in the thermal performance is observed, being F1 the case with highest stored energy of all, while F2 being worse than most and only better than cases A, B1 and D. This difference in output reflects the sensibility of thermal storage with the composition of the filler materials, and more specifically, with their fusion temperatures. Although F1 stores a higher amount of energy than cases C1 and C2, its efficiency in the utilization of the thermal capacity is lower than both.

Regarding the efficiency in the use of the thermal capacity, the best of all cases is C1: a multi-layered solid-PCM storage system. Total stored energy is around 90% of the best case in this aspect (F1), using much less PCM. Assuming that the cost of the encapsulated PCM should be higher than those of both the solid filler material and the HTF, it is expected that the cost-effectiveness of this multi-layered case is the best of all the cases containing PCM. The cost-effectiveness compared against a “pure” thermocline will depend highly on the cost of the encapsulated PCM. In any case, the convenience of the adoption of one configuration or another would need a further cost

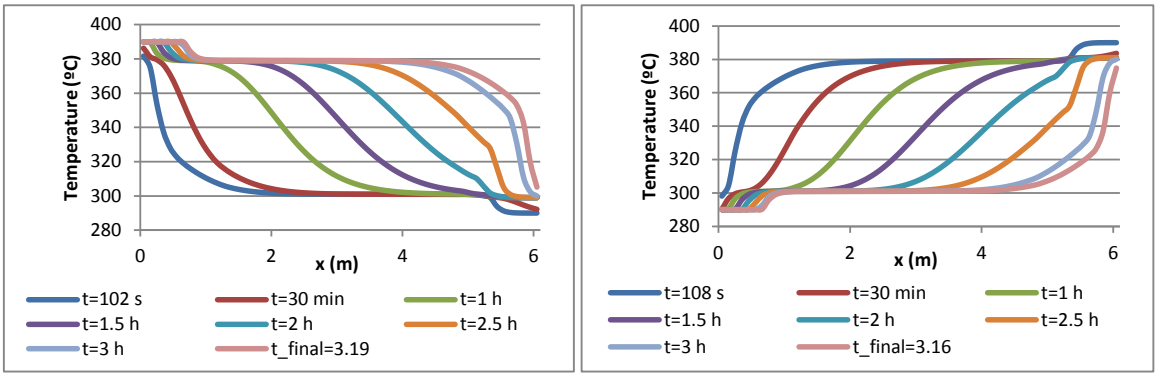

Fig. 5. Case C1 (multilayered solid-PCM). Fluid temperature maps at various instants. Left: Charge process. Right: Discharge. The abscissa indicates the distance from the fluid inlet (top of the tank for the charge and bottom for the discharge).

analysis, among other technical and non-technical issues.

Pressure losses due to the presence of the filler material are below 200 Pa for all the cases studied. The highest losses are present in the pure thermocline system, due to the higher compactness of the solid filler material compared to that of the encapsulated PCMs. However, when compared against the pressure differences arising due to height of the bed ($\rho gh \sim 1.1\text{x}10^5$ Pa) these represent less than 0.2% in all the cases, and hence, are negligible.

Numerical tests have been performed for several cases which have not been included in this work. For each combination of materials, variations in the proportions were carried out. Generally, results presented here are among the best obtained for each combination, except from some particular cases –which were chosen in order to show their bad performance– intended to be used comparatively. However, the presented set of cases is not exhaustive, i.e. there could be other configurations –for each combination of filler materials– with better performance.

5. Conclusions

A new multi-layered solid-PCM thermocline-like thermal storage concept for CSP plants has been presented. The key aspect of this new concept is the inclusion of PCM layers at both ends of the tank, whose fusion temperatures are conveniently chosen to be inside the "admissible" temperature ranges for the outlet of both charge and discharge processes. These admissible temperature ranges are defined by the requirements on the temperature of the fluid coming into the power generation block and into the solar receivers. The PCM layers act as thermal buffers, causing the outlet fluid to remain close to their fusion temperatures, and therefore inside the admissible temperature range for the corresponding process.

In order to design and evaluate the performance of such storage devices, as well as of the other thermocline-like systems considered, a numerical model has been implemented. This model has been successfully validated against experimental data.

Simulations have been run for a "pure" thermocline tank, tanks filled with a single PCM, multi-layered solid-PCM and cascaded-PCM arrangements. The obtained results show that the new multi-layered solid-PCM approach prevents from the high thermocline degradation presented by the pure thermocline, resulting in a much higher efficiency in the use of the overall thermal capacity of the system. Furthermore, compared against the cascaded-PCM concept, this new approach has the advantage of using much less encapsulated PCM for almost the same total stored energy, again with a higher thermal efficiency. Therefore, multi-layered solid-PCM thermocline storage system is a promising solution for its use in CSP plants.

Acknowledgements

This work has been financially supported by the *Ministerio de Economía y Competitividad, Secretaría de Estado de Investigación, Desarrollo e Innovación*, Spain (ENE-2011-28699); by the EIT through the KIC InnoEnergy project (ref. 20_2011_IP16); by the *Secretaria d'Universitats i Recerca (SUR) del Departament d'Economia i Coneixement (ECO) de la Generalitat de Catalunya* and by the European Social Fund.

References

[1] Py X, Calvet N, Olivès R, Echegut P, Bessada C, Jay F. Thermal storage for solar power plants based on low cost recycled material. EFFSTOCK, the 11th International Conference on Thermal Energy Storage 2009.

[2] Pacheco JE, Showalter SK, Kolb WJ. Development of a molten-salt thermocline thermal storage system for parabolic trough plants. J Sol Energy Eng 2002; 124(2): 153-159.

[3] Michels H and Pitz-Paal R. Cascaded latent heat storage for parabolic trough solar power plants, Solar Energy 2007; 81: 829–837.

[4] Wakao N, Kaguei S, Funazkri T. Effect of fluid dispersion coefficients on particle-to-fluid heat transfer coefficients in packed beds. Chem. Eng. Sci. 1979; 34: 325-336.

[5] Holdich RG. Fundamentals of particle technology. United Kingdom : Midland Information Technology and Publishing; 2002.

[6] Felix Regin A, Solanki SC, Saini JS. An analysis of a packed bed latent heat thermal energy storage system using PCM capsules: Numerical investigation. Renewable Energy 2009; 34: 1765-1773.

[7] Xu C, Wang Z, He Y, Li X, Bai F. Sensitivity analysis of the numerical study on the thermal performance of a packed-bed molten salt thermocline thermal storage system. Applied Energy 2012; 92: 65-75.

[8] Zavoico AB. Solar power tower design basis document. Sandia National Laboratories. Report no. SAND2001-2100; 2001.